Project Summary

Overview Swimming cells are integral to numerous environmental, human health, and engineering processes including bacteria in biodegradation, sperm in reproduction, and microalgae in biofuel production. Their natural and man-made environments are typically characterized by complex flows through heterogeneous media that remain poorly understood. This collaborative research project aims to determine the physical mechanisms governing the transport and chemotaxis of swimming cells in porous media flows through a rigorous combination of experiment and theory. Using microfluidic devices to engineer well-controlled porous environments, the two PIs will investigate the effects of microstructure (shape, porosity, ordering) and flow on cell transport for both dilute and dense suspensions of bacteria, human sperm and biflagellated microalgae, covering a range of canonical swimming styles and body shapes. Furthermore, the PIs will quantify how porous media structure modifies the transport coefficients of chemotaxing cells in chemical gradients. High-speed video microscopy of microbial suspensions will provide (*i*) a statistical characterization of large cell ensembles, and (*ii*) a mechanistic cell-scale view of the flagellar and hydrodynamic interactions mediating large-scale behaviors. Continuum and particle-based models will be implemented using state-of-the-art numerical techniques, and will be systematically validated against experiments to establish a quantitative, predictive framework for active cell transport in porous media flows.

Intellectual Merit In addition to their relevance in biology, genetics, and ecology, motile microorganisms have now become established models for biomechanics and locomotion in low Reynolds number flow, as they represent one of the few experimentally tractable model systems for non-equilibrium statistical mechanics. Swimming cells and recently developed, synthetic self-propelled particles comprise an emerging class of 'active' suspensions, whose transport properties take a significant departure from those of classical passive scalar and particulate flows. Due to their intrinsic non-equilibrium character, the modeling of active suspensions necessitates an extension of traditional transport concepts, requiring new theoretical approaches that must be implemented numerically and tested experimentally. Through the detailed comparison of theory with experimental data, the proposed research will identify and establish new classes of mathematical models to describe active non-equilibrium transport in complex structured environments, thereby advancing the quantitative understanding of essential biological, ecological, and technological processes.

Broader Impacts Swimming cells are pervasive throughout many facets of our lives. The work proposed here could have broad societal implications for public health by leading to technologies that provide clean drinking water, stifle bacterial infection, and mediate infertility. The collaborative award will foster the interdisciplinary training of two Ph.D. students at the intersection of biology, physics, and engineering. By virtue of the close proximity of MIT and Tufts, theorist and experimentalist will work together closely throughout their training to promoting collaboration and communication, both of which are essential skills for the next generation of interdisciplinary scientists and engineers. The MIT Ph.D. student (Dunkel) will participate in the MIT PRIMES program as a graduate mentor to an outstanding high school student in a rigorous after-school research program at MIT. This program develops mentoring and teaching skills for the graduate student and exposes promising high school students to new areas of STEM. The PIs will capitalize on the visual nature of this project to broadly disseminate their results through existing channels that promote STEAM, including the Cambridge Science Festival, Tufts Research Visualization Awards, and APS-DFD Gallery of Fluid Motion. The PIs have consistently published in leading scientific journals and their work has been highlighted in popular press outlets such as *BBC News*, *Nature News and Views*, and *Physics Today*, thereby reaching a large public audience.

Project Description: Transport and Chemotaxis of Swimming Cells in Porous Media Flows

1 Introduction

Swimming cells (Fig. 1A-C) play important roles in ecology [1] by recycling organic matter [10, 36], in human health through reproduction [30] and the spread of infection from biomedical devices [11], and in engineering applications including bioreactors and bioremediation [2, 34]. In addition to living in ubiquitously dynamic fluid habitats, motile cells often thrive in confined porous environments (Fig. 1D-F). Together with engineered self-propelled particles [45], swimming cells comprise a class of 'active' suspensions, presenting a host of unique experimental and theoretical challenges to the fields of multiphase and particulate flows. Self-propulsion, morphology, and biological behaviors generate unique interactions with flow, surfaces, and other cells. Due to this complexity, a quantitative description of the transport properties of swimming cells under realistic conditions is lacking, especially in porous media flows (Fig. 1D-F). Through a close collaborative effort between two PIs at MIT and Tufts, we propose to study the microscopic and continuum-level transport of swimming cells in porous media, through a combination of microfluidic experiments and theory.

Motility enables cells to seek out resources including nutrients, light, and mates for survival [23], an ability conferred through thin, actuated flagella. Individual cells (1-10 μm) typically have one or several flagella ranging in length from 5-50 μm [6] (Fig. 1). Flagella are categorized as one of two types: (*i*) Prokaryotic cells including bacteria have rigid, helical filaments ($\approx$20 nm diameter), which are actuated at the base by a single rotary motor embedded in the cell membrane. (*ii*) Eukaryotic cells including sperm and microalgae have flexible flagella ($\approx$200 nm diameter), which are actuated along the length of the flagellum by dynein motors [6]. Flagella are additionally utilized in one of two general but distinct swimming styles including cells with anterior flagella that pull their bodies through the fluid ('pullers'), and cells with posterior flagella that push their bodies through the fluid ('pushers') [39]. In bulk fluid, cells often swim in persistent random walk motility patterns [4, 48, 57], where otherwise straight-line swimming ('run') is augmented by discrete, flagellar-induced turns ('tumbles') or rotational Brownian motion [3]. Motility patterns are strongly affected by the flow [52], surfaces [29, 63], and other stimuli such as light [14] and gravity [47]. Many species respond to spatial gradients of dissolved chemical species, including nutrients and oxygen, which bias their random walks and guide cells to these resources [4].

The vast majority of cell motility studies to date have focused on swimming in bulk, quiescent fluids far from surfaces [23], but the natural environments of many swimming cells are characterized by complex fluid flows through porous, microstructured materials. For example, marine bacteria, which play a key role in biogeochemical cycling [1, 36], thrive in porous aggregates such as marine snow (Fig. 1D). These fractal-like detritus agglomerations span up to several centimeters in size [9], providing a nutrient-rich habitat for cells as they settle through the water column [43]. Human parasites swim through blood flow [61] in complex vascular networks to spread infection. In the female reproductive tract, motile sperm swim through biopolymer networks in cervical mucus [53] (Fig. 1E) and complex tissue topology in the reproductive tract, all while subject to significant ciliary and peristaltic flows [19]. Swimming bacteria are used for bioremediation of oil and chemicals in porous soils [34, 10]. Microalgae cells are exposed to flow during cultivation and processing for biofuel production [2], and require porous glass microstructures for light distribution and efficient cell growth (Fig. 1F) [26]. These natural and man-made systems encompass a multitude of biological

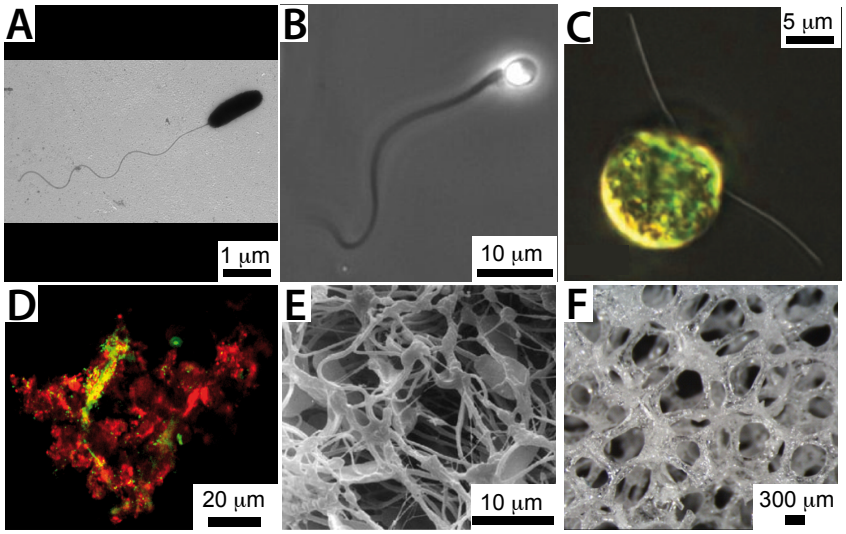


Figure 1: Motile single cells experience natural and engineered porous, fluid environments. Swimming cells (top row): **A** uniflagellated marine bacterium, *Vibrio alginolyticus* [56], **B** human sperm (credit: J.S. Guasto), **C** biflagellated, photosynthetic algae, *Chlamydomonas reinhardtii* (credit: K. Drescher) [23]. Porous environments (bottom row): **D** confocal section of organic marine aggregate (green is nucleic acid, red is glycoconjugates) [43], **E** bovine spermatozoa in vaginal fluid [53], and **F** engineered glass sponges for light distribution in photobioreactors [26].

cell types, cell swimming styles, and porous microstructures.

While theories for passive scalar and particulate transport in porous media flows are well established, swimming cells have several prominent biophysical traits that distinguish them from their passive counterparts [23]:

1. *Self-propulsion* enables relatively large, non-Brownian cells to cross fluid streamlines unlike passive particles of similar size. While the random walks of swimming cells draw comparison to the molecular diffusion of passive scalars, this analogy rapidly breaks down in non-trivial cases due to the far-from-equilibrium nature of cell motility [7].
2. Cell-cell interactions lead to *collective motions* of swimming cells in dense suspensions, forming dynamical structures many times larger than the scale of a single cell [37, 16] (Fig. 2).
3. *Elongation* is ubiquitous among motile bacteria and sperm, strongly coupling orientation to flow [27]. When combined with self-propulsion, elongation leads to heterogeneous spatial distributions of cells [35, 52], a phenomenon not exhibited by spherical or passive particles alone (Fig. 3).
4. Motile cells exhibit strong *surface interactions* due to the steric [41] and hydrodynamic [5] forces on actuated flagella, resulting in complex surface scattering behaviors (Fig. 4) [28].
5. *Chemotaxis* and other active sensing mechanisms enable cells to direct their motility in a non-random fashion, rectifying their otherwise diffusive spreading (Fig. 7) [4].

Significant progress has been made in recent years to understand these individual, isolated phenomena, but how these mechanisms collectively contribute to the bulk transport properties of active cell suspensions in porous media flows is not understood [59].

We propose to develop an empirical, microscopic description of the biophysical mechanisms mediating cell transport at the level of single cell mechanics, through precisely-controlled microfluidic experiments in porous media analogs. These experimental results will contribute the necessary level of detail to build both discrete and continuum theoretical models of active cell transport. Taken together, the proposed collaborative research will provide the necessary quantitative tools to analyze swimming cell suspensions in ecologically and medically relevant scenarios, and to systematically engineer both natural and synthetic active suspensions.

2 Specific Aims and Objectives

The goal of this collaborative project is to determine the biophysical mechanisms governing the transport of individual swimming cells and dense cell suspensions in porous media flows, as relevant to biodegradation in ecological systems and transport processes within the human body. To achieve this objective, we pursue a synergistic approach based on a close collaboration between experiments and theory. Highly-resolved empirical data will allow us to develop and constrain theoretical models, reciprocating the formulation and testing of new hypotheses for the dynamics of active suspensions in microstructures. We will measure and compare the characteristic transport properties of three important classes of single cells with starkly differing swimming strategies that live in porous environments, such as soil or the human body, and utilize external fields for navigation: (*i*) bacteria, (*ii*) human spermatozoa and (*iii*) green micro-algae. Microfluidic devices will provide unprecedented control of the physical and chemical environmental landscape, and high-resolution video microscopy will yield quantitative information on how physical interactions with microstructure at the single-cell scale affect macroscopic, bulk transport properties. These experiments will provide guidance for, and be guided by, detailed theoretical modeling using state-of-the-art numerical techniques. Specifically, our joint efforts focus on three key aims:

1 Establish how microstructure in porous media affects the motility of individual swimming cells

- 1.1 Characterize how the persistent random walks of single *Bacillus subtilis* bacteria, sperm cells and *Chlamydomonas reinhardtii* algae are modified in porous media, as compared to free space, by using microfluidics to control the (*i*) porosity, (*ii*) size, (*iii*) shape, and (*iv*) spatial distribution of obstacles in a microstructured environment.
- 1.2 Determine how physical mechanisms, such as steric and hydrodynamic interactions of single cells with porous microstructure, govern changes in single cell transport.
- 1.3 Develop an individual-based model of cell motility in porous media.

2 Identify how porous media affect transport in dense microbial suspensions

- 2.1 Using microfluidic experiments, quantify how the onset of collective motion in bacterial suspensions with increasing cell concentration is modified by microstructured environments.
- 2.2 Extend existing continuum models of dense bacterial suspensions to porous media environments.
- 2.3 Theoretically predict and experimentally determine how statistical properties (order/disorder) and confinement in porous media enhance or reduce transport in dense cell suspensions.

3 Determine the combined effects of porous media flows and chemoattractant gradients on the transport of swimming cells

- 3.1 Using precise microfluidics and individual cell models, determine the impact of externally imposed fluid flow through porous microstructure on the transport of single swimming cells.
- 3.2 Combine experiments and modeling to determine how porous microstructure affects the biased random walks of swimming cells and their ability to navigate chemical signal gradients.
- 3.3 Theoretically predict and experimentally demonstrate optimal obstacle structures and flow regimes that promote or diminish the chemotactic response of swimming cells for a given media porosity.

3 Background and Preliminary Results

Collective swimming in unconfined geometries Recent experimental and theoretical work by the PIs [62, 16] and others [33, 12, 55] showed that the interplay of hydrodynamic and steric alignment interactions between individual cells can lead to large-scale collective dynamics in bacterial suspensions (Fig. 2A-D). The coordinated motion of such pusher cells can substantially modify the transport properties in the underlying fluid, as evidenced by the enhanced diffusion of tracer particles [64] and an effective viscosity reduction at intermediate-to-high bacterial concentrations [55]. An intriguing feature of collective dynamics in dense bacterial suspensions is the emergence of a characteristic vortex size ($\sim 50 - 80\,\mu$m; Fig. 2C), facilitating the stabilization of collective motion in confinement (Fig. 5). In the opposite case of puller swimmers, PI Guasto and collaborators [40, 38] were able to show that even small concentrations of *Chlamydomonas* microalgae can significantly enhance diffusive transport in the surrounding medium (Fig. 2E-H). In contrast to elongated bacterial pusher swimmers, however, these algae were found to increase the shear viscosity [49], illustrating that different swimming strategies can affect the bulk mechanical properties of cell suspensions.

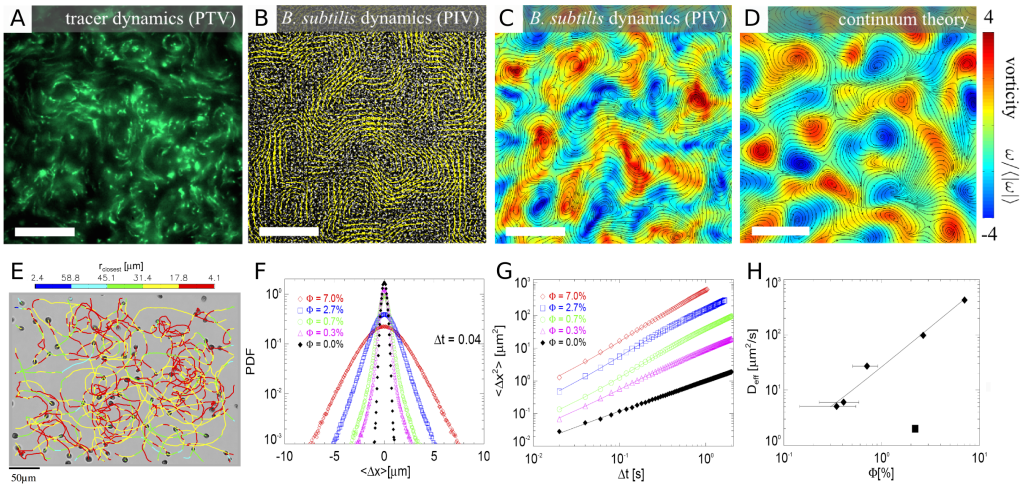


Figure 2: Collective microbial dynamics affects diffusive material transport and fluid mixing. **A** Meso-scale turbulent dynamics of fluorescent tracer particles reflects the collective dynamics (**B**) in a dense pusher (*B. subtilis*) suspension [16]. Scale bars 50 μm. **C** The vorticity field reveals the characteristic scale of the collective bacterial dynamics. **D** Numerical simulations of a continuum theory developed by PI Dunkel and collaborators [62, 15] quantitatively reproduce the main features of the bacterial velocity field. **E** Tracks of puller swimmers (*Chlamydomonas*) in a semi-dilute suspension [38]. **F** The tracer displacement distributions broaden significantly with the algal concentration (volume filling fraction Φ). **H** The associated tracer diffusion constant increases linearly with the algal filling fraction, signaling that diffusive transport (**G**) in the fluid is strongly enhanced by the swimming microalgae.

Swimming in shear Cells ubiquitously live in flowing fluid environments [23]. Shear-induced hydrodynamic forces and torques on cells interact with asymmetric body weighting [32] and helical flagellar shapes [44] to generate local cell accumulations in both laminar [18] and turbulent [17] flows. PI Guasto and co-workers recently showed that even simple, elongated cell body shape [35], which is typical of bacteria and sperm [6], is sufficient to generate complex motility patterns in shear (Fig. 3B) and strong spatial heterogeneity in cell concentration (up to 70% decrease; Fig. 3C) [52, 66]. Shear-induced cell rotation ('Jeffery orbits' [27]) aligns elongated cells with the flow direction in

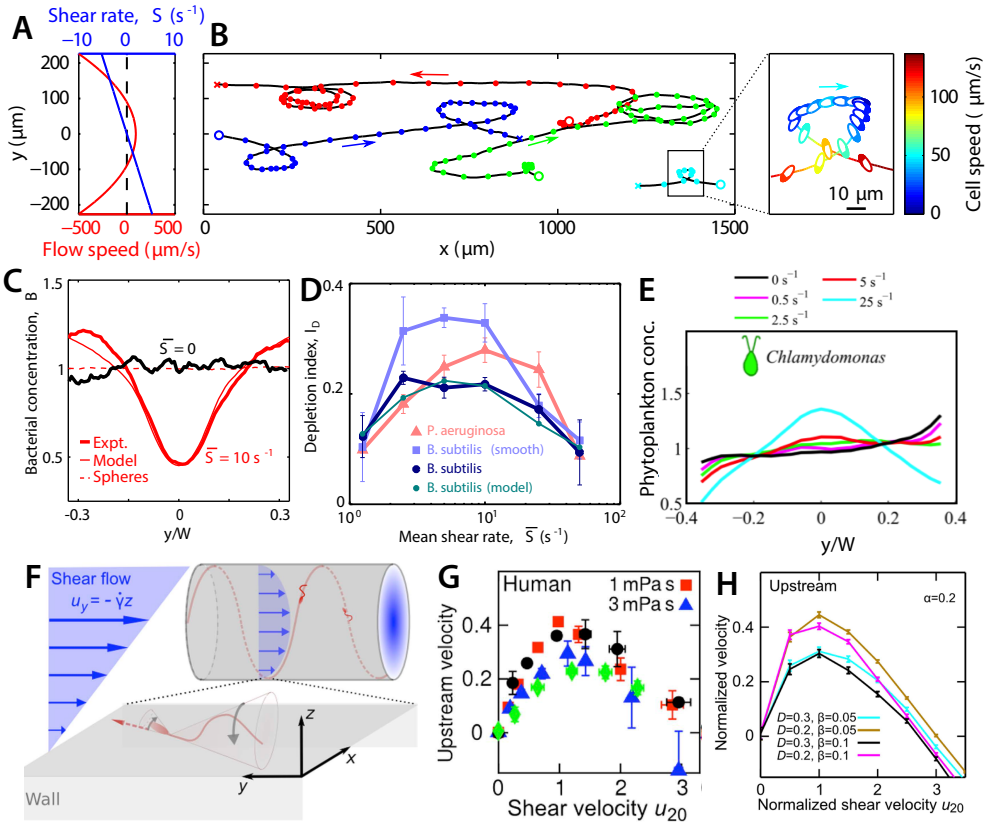


Figure 3: Fluid shear affects the motility of swimming bacteria, sperm, and microalgae. **A-D** Microfluidic experiments demonstrating that shear (**A**) generates complex motility patterns of what (**B**) [52]. **C** Nonuniform shear drives cell depletion from low shear regions and accumulation in high shear regions. **D** Cell depletion is maximal at physiologically and environmentally important shear rates ($\approx$10 s^{-1}) for a range of bacterial species and swimming styles. **E** In contrast to bacteria, biflagellated microalgae accumulate in low shear due to their effectively oblate shape [Barry, et al., *submitted* (2014)]. **F-H** Sperm cells accumulate at solid interfaces due to steric and hydrodynamic interactions with walls [28]. In shear, the hydrodynamic torque on the $\approx$50 μm-long flagellum maintains cell orientation upstream (**F**), guiding cell motility. The strength of the upstream alignment and the downstream advection compete, resulting in a maximal guided swimming speed and confirmed by simulations of the flagellar interactions with shear (**H**).

high shear regions, reducing their mobility across the channel and effectively trapping the cells. This effect is reversed for oblate microalgae (Fig. 3E). Shear-induced rotation competes with random cell motility in a complex way, maximizing cell heterogeneity at environmentally and physiologically relevant shear rates (2-10 s^{-1}; Fig. 3D). Many swimming cells exhibit strong interactions with solid surfaces, which are further modified by ambient flow. PI Dunkel and co-workers demonstrated [28] through microfluidic experiments combined with simulations that the shear-induced hydrodynamic torque on sperm cells, combined with their attraction to solid surfaces, can rectify sperm swimming orientation in the upstream direction (Fig. 3F). Upstream cell alignment increases with increasing shear rate, but upstream swimming speed is deteriorated by advection in the opposite direction. The competition between alignment and advection results in optimal guided motility at shear rates relevant to female reproductive tract physiology ($\approx$1 s^{-1}; Fig. 3G-H). It is not known how complex flow topologies or microstructured surface topologies modify the transport coefficients of single swimming cells over larger scales, for example in porous flow networks.

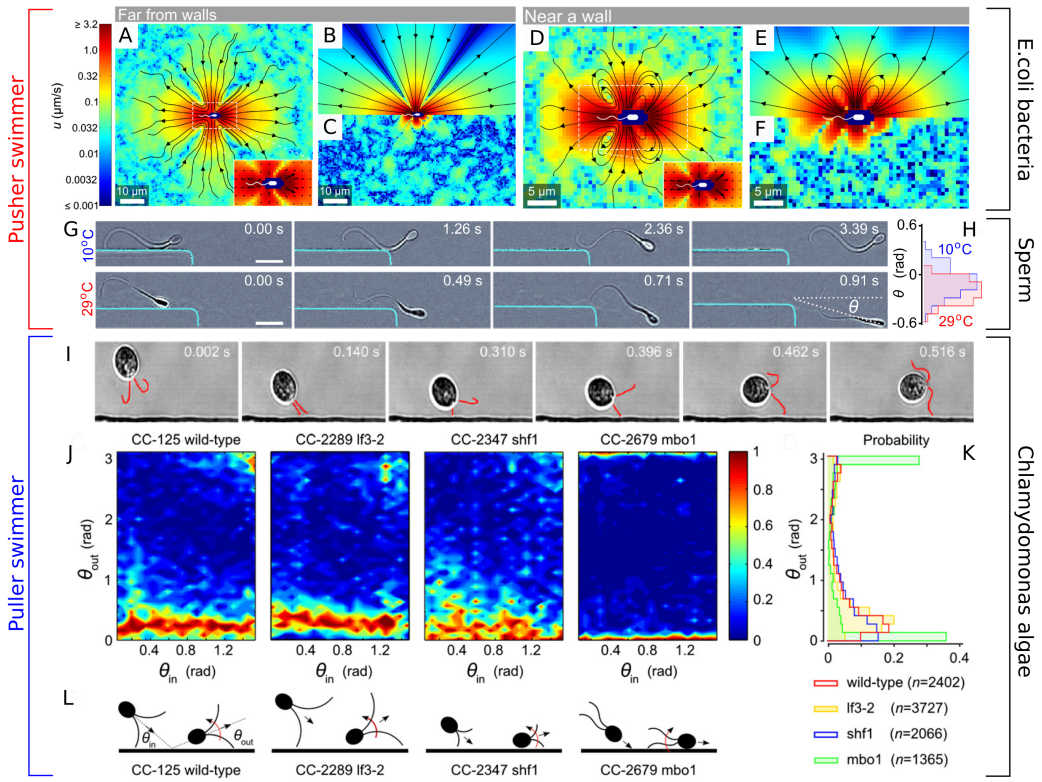


Figure 4: Microbial pusher and puller swimmers exhibit qualitatively different surface scattering laws. The time-averaged flow [13] of an *E. coli* bacterium (**A**) is well described by a symmetric pusher-type force-dipole flow (**B**) plus a small anisotropic residual component (**C**). Close to a solid no-slip surface, the flow topology changes (**D-F**), and the flow magnitude decays more rapidly with increasing distance from the cell body. **G** Similar to bacterial pusher-swimmers, sperm cells also become effectively trapped at channel boundaries [29, 28], as near-field hydrodynamics and elastic flagellar interactions with the surface result in a negative mean scattering angle (**H**). **I-L** By contrast, biflagellate puller-swimmers (*Chlamydomonas*) depart at a practically constant positive angle from the surface; only the backwards-swimming pusher-mutant CC-2679 mbo1 becomes trapped at the boundary. Taken together, these findings suggest that puller and pusher organisms will behave very differently in a porous medium.

Effects of boundaries on individual microswimmers Seminal earlier studies investigated microbial suspensions under idealized conditions, but very little is known about how complex porous structures affect swimming microbes. Preliminary experimental evidence suggests that physical boundary conditions can substantially affect individual [13, 29, 28] and collective [63] cell locomotion. In 2011, PI Dunkel and collaborators [13] reported the first direct measurements of the mean bacterial flow field near and far from boundaries. This study revealed that a nearby no-slip surface can substantially alter the fluid flow around a swimming bacterium (Fig. 4A-F). In subsequent work [29] that compared the scattering of individual pusher and puller swimmers from solid boundaries, PI Dunkel and colleagues found that mammalian sperm (Fig. 4G,H) and *Chlamydomonas* algae (Fig. 4I-K) exhibit qualitatively different surface scattering laws (Fig. 4H,K), reflecting the different swimming strategies and flagellar beat geometries [29]. These results, combined with the fact that the flagellar beat amplitude can be tuned through thermal and chemical stimuli, suggests the possibility to design artificial porous media that can separate different microbial species.

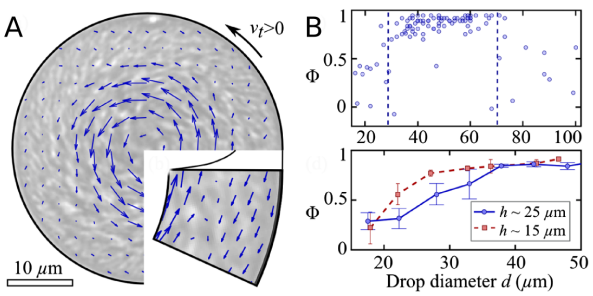


Figure 5: Confinement can stabilize collective microbial swimming. **A** Transient vortex structures in unconfined bacterial suspensions typically decay after a few seconds [16], whereas bacteria confined in an oblate droplet self-organize into a stable helical vortex [63] driven advective currents that are created by a thin counterrotating boundary layer of cells. These findings corroborate the important role of confinement-induced boundary conditions. **B** Analysis of the vortex order parameter suggests that collective bacterial motion through a porous medium is sensitive to the pore-size distribution.

Effects of boundaries on collective swimming PI Dunkel and collaborators [63] showed that boundaries can stabilize collective bacterial vortex motion for several minutes, whereas the typical coherence time-scale in an unconfined bacterial bulk fluid is of the order of just a few seconds [16]. The robust boundary-induced stabilization occurs if the typical scale of the confining volume becomes of the order of the characteristic vortex size of a bulk suspension (Fig. 5). Their study [63] further revealed that the coherent bulk dynamics of the bacteria is largely controlled by a thin self-organized bacterial boundary layer. This layer is formed by bacteria that push against the enclosing solid surfaces, thereby creating a strong advective back flow that dominates the effective cell velocity in the bulk. Although these experiments [63] focussed on idealized spherical boundary geometries, it is plausible to assume that qualitatively similar effects occur in natural porous materials. Since diffusive transport is enhanced by collective bacterial swimming [64], one can hypothesize that boundary-induced coherent bacterial dynamics can substantially affect material transport through a porous medium when the typical pore size is of the order of $50-100\,\mu$m.

Chemotactic motility in flow Directed cell swimming due to chemical signal gradients ('chemotaxis') [60] and light ('phototaxis') [47] has long been known to induce pattern formation in cell suspensions due to coupling with gravity and collective, self-induced flows. Investigations into the effects of externally-imposed flow on chemotaxis at the level of individual swimming cells are rare and limited to simple shear flows in both theory [42] and experiment [51]. Using novel microfluidic devices engineered to independently control oxygen gradients and fluid flow (Fig. 7A), PI Guasto and coworkers demonstrated that the chemotactic performance of the oxygen-seeking bacterium *B. subtilis* (Fig. 7B) is significantly hampered by non-uniform fluid shear in a Poiseuille flow (Fig. 7C). In quiescent conditions, *B. subtilis* strongly accumulated in the oxygen-rich region of the microchannel,. The chemotactic ability of the cells decreased with increasing mean shear rate, which was suppressed by up to 85% (Fig. 7C, inset), due to trapping in high-shear zones near the walls (Fig. 3). These results demonstrate that heterogeneous hydrodynamic environments can suppress the directed, chemotactic motility of swimming cells. However, it is not known how flow complexity and porous media structure modify the biased random walks of single cells.

Summary Much has been learned about the fundamental interactions between swimming cells and their physical environments under highly idealized laboratory conditions, but little is understood about how the interplay between porous media structure, fluid flow and chemotaxis affects microbial locomotion under natural condition. To address this issue, we will fabricate heterogeneous, yet precisely-controlled, microfluidic devices to serve as realistic analogs to the ubiquitously complex, porous environments in which swimming cells live. These experiments will be complemented, rationalized and guided by detailed quantitative theory.

4 Proposed Work

Aim 1.1 Characterize the persistent random walks of single cells in porous media Our previous work [29] showed that interactions of otherwise straight-swimming cells with flat, solid boundaries generate isolated reorientation events that depend on swimming style and flagellation (Fig. 4). Here, we will examine how successive surface collisions in a porous medium affect transport of three cell types with distinct swimming styles: bacteria (*B. subtilis*), sperm (human), and microalgae (*Chlamydomonas*). The 'run-and-tumble' motion of cells with mean swimming speed u, persistence ('run') time τ, and mean reorientation ('tumbling') angle $\langle\cos\theta\rangle$ is characterized by an effective diffusivity $D = u^2\tau/[3(1 + \langle\cos\theta\rangle)]$ [3]. Porous media have two routes to modify cell transport coefficients: When the typical pore diameter s is smaller than the persistence length $\ell = u\tau$ of the cell's random walk, microstructure-induced turning events reduce τ and, hence, D. Moreover, surface interactions augment the turning angle, thereby modifying transport coefficients through changes of $\langle\cos\theta\rangle$. Thus, depending on the details of the cell-surface interactions (Fig. 4), cell motility could be either rectified [20, 29] or further randomized in porous environments.

To experimentally model porous structures having length scales relevant to biological and engineering processes (Fig. 1), we will design and fabricate microfluidic devices (see methods section below) with arrays of pillar-like obstacles (Fig. 8A-C). Obstacle size, shape, order, and porosity will be accurately varied with a resolution <5 μm. Using video microscopy and high-resolution cell tracking methods (Fig. 8D), we will quantify the random walks of the three model swimmers (>1000 cells) through metrics including u, τ, θ and D, using free-swimming cells far from boundaries as a benchmark. Shape and size effects will be measured for convex and concave obstacles, to establish scattering laws for each cell type and obstacle shape as function of impact angle and impact parameter. The obstacle radius R will be systematically varied in the range $a \leq R \leq 10a$, where a is the typical cell size (for *Chlamydomonas* $a \approx 5$ μm). Empirical scattering laws will provide critical data for simulations, which will reciprocate testable predictions (Aim 1.3) of the porous geometries most affecting transport, which we expect in the range $s \leq \ell$. Transport coefficients will be measured for a range of lattice dimensions ($s = \ell$, $\ell/3$, and $\ell/10$). Finally, a distinct advantage in using model cells is our ability to explore variations in fundamental physical and behavioral cell attributes on their transport through genetic mutants, including a non-tumbling *B. subtilis* strain.

Aim 1.2 Determine the microscale physical mechanisms governing single cell transport The relative importance of hydrodynamic and steric forces in bacterial cell-surface and cell-cell interactions has been hotly debated in recent years [5, 41]. For eukaryotic cells, recent work [29] by PI Dunkel and collaborators showed that steric flagellar interactions with flat surfaces play a larger role than previously thought (Fig. 4G-K). Yet, it is not understood how complex flagellar dynamics and flow (Fig. 4A-F) [13] generated by swimming cells interact with micron-sized, high-curvature solid structures. We will quantify the relative contributions of hydrodynamic and mechanical interactions between swimming cells and microstructured obstacles, using high-speed imaging (1000 fps) to capture the fast flagellar beating (≈50 Hz) and the associated flow. For all three model organisms, we will perform complementary experiments to Aim 1.1, using sparsely distributed obstacles ($s \gg \ell$) to measure the unsteady fluid flows [21] generated during cell scattering events. High spatiotemporal resolution of the flow field will enable us to infer the hydrodynamic forces and torques acting on cells during these interactions. Similarly, high-speed video of the flagellar dynamics of sperm and *Chlamydomonas* during scattering events will determine the steric force contribution for all obstacle geometries described in Aim 1.1.

Aim 1.3 Develop an individual-based model of cell motility in porous media In support of Aims 1.1-2, the Dunkel group will implement two theoretical approaches:

(*i*) Within the persistent random walk (PRW) framework, the locomotion of cells is modeled as a discrete non-Markovian RW in position space that can be mapped onto an equivalent Markov process in a higher dimensional phase space. The input parameters of this model are the lattice geometry, reflecting the structure connectivity of the porous medium (Fig. 8), and the transition probabilities, determined from the experiments (Guasto group). An advantage of this discrete, stochastic modeling approach is the existence of established mathematical results for mean first passage times, yielding predictions that can be directly compared with experiments. In preparation of the proposed project, an undergraduate student (MIT Summer Research Program) advised by a 2nd year PhD student in the Dunkel group, has successfully implemented a preliminary version of this model for a cubic lattice. During year 1 (Table 1), the PhD student will extend this framework to general lattice structures, to represent those realized in our experiments.

(*ii*) Within the continuous-time Langevin approach, individual cells will be represented as point-like particles with position vector $\boldsymbol{X}(t)$ and orientation vector $\boldsymbol{N}(t)$. The dynamics of these coordinates is governed by over-damped stochastic differential equations, as previously implemented by PI Dunkel to study sperm locomotion near boundaries in shear flow [28]. The translation of the position vector $\boldsymbol{X}(t)$ is determined by the cell's self-swimming velocity $u\boldsymbol{N}$. The organism-dependent re-orientation dynamics $\boldsymbol{N}(t)$ is determined by a stochastic tumbling contribution and interactions with the porous medium. The scattering of swimmers from obstacles will be incorporated into the Langevin model by implementing the experimentally measured [29] inelastic collision rules (Fig. 4H,J) relative to the tangential plane at the contact point (Fig. 7E,F). Direct numerical simulations of this model will produce detailed trajectory data that will be directly compared against the corresponding experimental particle-tracking data collected in the Guasto lab.

Aim 2.1 Quantify the onset of collective cell motion with concentration in porous media Collective motility [12, 55] in bulk microbial suspension can substantially enhance advective and diffusive transport in the surrounding fluid [64, 40, 38]. Recent work by PI Dunkel and co-workers [63] showed the collective bacterial dynamics can be stabilized by boundary interactions if the confinement length scale is of the order of the dynamical bulk correlation length 50-100 μm (Fig. 5). Here, we will determine whether the porous microstructure can suppress (promote) the onset of collective *B. subtilis* motion. Because single cells cannot be resolved in dense suspensions, the fluid-like collective motion will be characterized by the unsteady flow field of the cells using well-established particle image velocity methods (micro-PIV). Statistical measures of the bacterial flow field, including spatial and temporal velocity correlations, will characterize the degree of collective motion for five cell concentrations around the bulk threshold concentration and will be compared with continuum-model predictions (Aim 2.2) for various geometries.

Aim 2.2 Extend continuum models of bacterial suspensions to porous environments To model the dynamics of dense suspensions in a porous medium, the Dunkel group will generalize and implement effective continuum models that couple the local microbial concentration field $b(t, \boldsymbol{x})$ and the mean microbial orientation vector field $\boldsymbol{P}(t, \boldsymbol{x})$ to the Stokes equations that describe the fluid velocity field $\boldsymbol{u}(t, \boldsymbol{x})$ in the porous medium (see methods section below for details). These models will be mathematically similar to those developed and successfully applied in previous work by PI Dunkel and collaborators [63], although the complex boundary structure of the porous medium poses additional theoretical and numerical challenges. Since our experimentals will realize

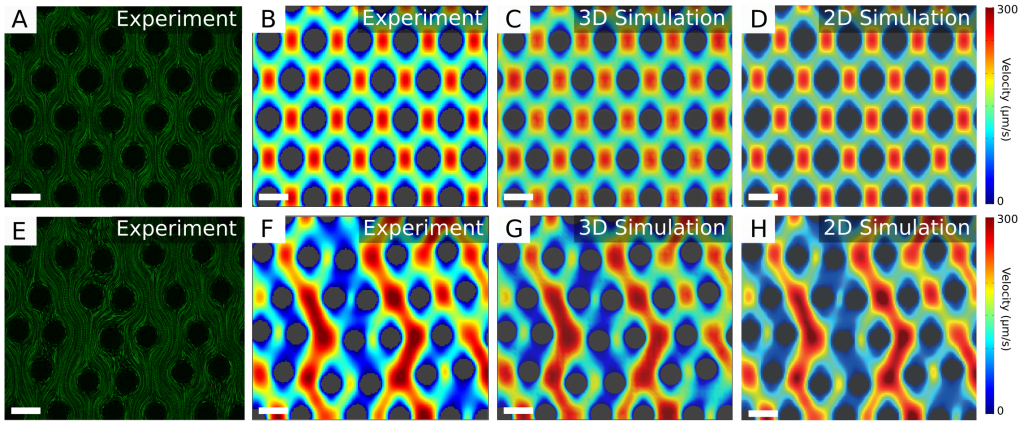


Figure 6: Small changes in the spatial structure of a porous medium can cause drastic changes in the hydrodynamic transport patterns. **A-D** Pressure-driven flow through an ordered lattice of obstacles as measured in our experiments and simulations at the channel midplane. Scale bars 30 μm. **E-H** When the obstacles are randomly displaced, fast transport lanes emerge. The very good agreement between the experiments, 3D Stokes simulations and 2D Hele-Shaw simulations confirms that our numerical framework produces accurate predictions.

quasi-2D porous media, we plan to focus on the numerical implementation of effective 2D models that account for the 3D microchannel structure through suitable effective penalization terms. As proof of principle, the Dunkel group has implemented a 3D Stokes solver that reproduces accurately the experimentally observed, pressure driven flow patterns (Fig. 6). Moreover, a Hele-Shaw-type reduction from 3D to 2D by averaging over the small vertical channel dimension was found to yield good quantitative agreement for the Stokes flow component of the model (Fig. 6D,H), promising a computationally efficient implementation of the full continuum model. This conceptually and numerically demanding task will be carried out by PI Dunkel.

Aim 2.3 Determine how confinement enhances or reduces transport in dense suspensions Active cells [64, 40, 38] greatly enhance the transport of passive particles and scalars, especially in the case of collective bacterial motion in dense suspensions, promoting the mixing of dissolved nutrients, gases, and signaling molecules throughout cell colonies [64]. Whether these active transport processes are enhanced or diminished by the presence of microstructured environments is unknown. For a range of bacterial concentrations and medium geometries (informed by Aims 2.1-2), we will characterize the relative enhancement of transport for passive, fluorescent tracer particles embedded in the bacterial suspensions. Particle tracking data will provide robust statistics for transport metrics, primarily characterized by an effective diffusion coefficient [40, 38].

Aim 3.1 Determine the impact of flow on swimming cell transport through porous media Porous media generate complex, shear-dominated flow patterns (Fig. 6), which we anticipate to severely augment cell motility and transport relative to the flow [52, 32, 18]. PI Guasto and coworkers recently demonstrated [52] that shear-induced flow alignment competes with effective rotational cell diffusion, D_R, to locally trap swimming cells in high shear zones causing striking heterogeneity in suspensions. However, the effects of shear (Fig. 3) on the random motion of single cells over large scales through complex, microstructured media are not known. We hypothesize that shear generated near no-slip obstacles will promote cell alignment with the flow direction and strongly inhibit cross-stream mobility. Focusing on circular obstacles, we will quantify cell spreading dynamics in porous microfluidic channels for both ordered and disordered microstructures, and

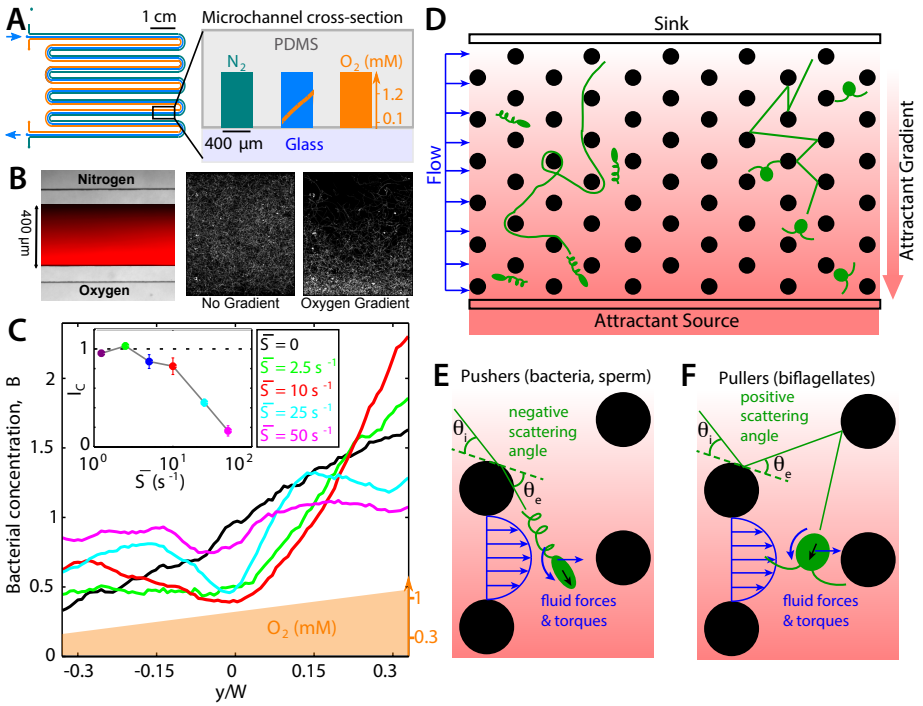


Figure 7: Microfluidic devices enable precise control of microstructure, flow, and chemical signals. **A** Engineered chemotaxis microchannel (right: cross-section), where oxygen diffuses through PDMS walls, generating a steady, linear oxygen gradient (**B**, left). Swimming bacteria (*B. subtilis*) accumulate in the high oxygen zone (**B-C**, right) [52], a phenomenon that deteriorates with increasing mean shear rate $\bar{S}$ (**C**). Inset: I_C is the normalized cell chemotactic ability, which decays with increasing $\bar{S}$. **D** Proposed porous media microfluidic device. **E-F** Differences in 'pusher' and 'puller' interactions with microstructure and flow can yield strong differences in their transport characteristics in porous media.

for various flow regimes, set by the rotational cell Péclet number $Pe_R = \bar{S}/D_R$ with mean shear rate $\bar{S}$ [52]. Due to their elongation, we expect bacteria and sperm to interact more strongly with local shear than the slightly oblate *Chlamydomonas*. We have already designed, fabricated, and characterized porous microfluidic devices in the Guasto group, which benchmarked hydrodynamic simulations by the Dunkel group (Fig. 6) that will be integrated with individual motility models. Similar to Aim 1, cell tracking will yield the mean transport coefficients of the motile sperm and bacteria in porous media, transverse to the flow direction. High-speed microscopy measurements will complement these experiments and determine how flow mediates cell interactions with solid obstacles. We will correlate local cell residence times in the channel to flow features dominated by rotation or extension, and determine the mechanisms hindering cell mobility [35, 66, 58].

3.2 Determine how microstructure modifies chemotactic cell motility A unique feature of swimming cells is their ability to sense and respond to chemical signals in their environment [4, 30] through active, flagellar-induced turning. PI Guasto and coworkers recently demonstrated that shear-induced cell rotation in flow confounds cell navigation by disrupting the cells' ability to independently control their orientation [52]. We hypothesize that reorientations generated by cell-surface scattering in a porous environment (Aim 1) will significantly modify the cells' ability to navigate chemical gradient signals, which might promote or diminish chemotactic ability depending on the nature of the cell-surface interaction. Focussing on the aerotactic bacterium *B.*

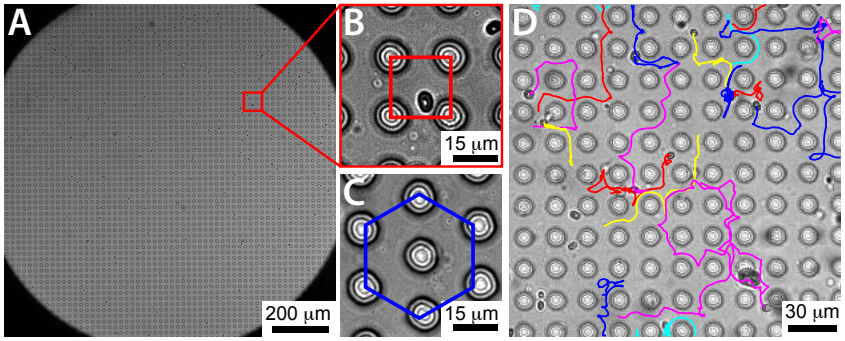


Figure 8: The motility patterns of *Chlamydomonas* are modified in porous media microfluidic environments. **A** Low magnification image of a porous media microfluidic channel (20 μm square lattice, 10 μm circular obstacles, 10 μm deep). **B** Square lattice and **C** hexagonal lattice. **D** *Chlamydomonas* cells exhibit highly tortuous measured trajectories due to interactions with the microstructured obstacles.

subtilis, PI Guasto will adapt recently-developed microfluidic technology for generating simultaneous, independently-controlled oxygen gradient and fluid flow [52] to the porous microchannels (Fig. 7). For select obstacle geometries and microstructure order, and informed by simulation, we will quantify the directed motility of the chemotactic bacteria through an ensemble averaged statistical approach using video microscopy. Bias in the cells' random walk adds a chemotactic drift to the cells' motion in the oxygen gradient, resulting in a ballistic component to the cells' mean-square-displacement over long times and providing the primary metric to judge the severity of microstructure effects on cell chemotaxis. Measurements of cell chemotaxis in the bulk (free from porous microstructure and flow) will benchmark these results, providing key parameters [31] for complementary simulations and experiments in porous media with and without flow (Aim 3.3).

3.3 Demonstrate how microstructure and flow promote or diminish chemotactic motility Our numerical framework allows us to efficiently simulate 3D Stokes/2D Hele-Shaw flow through a porous medium at spatial resolutions comparable to our experiments (Fig. 6). Preliminary tests show that even moderate randomness in the obstacle distribution produces strongly inhomogeneous flow patterns (Fig. 6E-H), that will substantially affect the transport of passive chemical and active microbial components through the medium. These simulations will allow us to systematically quantify the connection between porous media structure and fluid flow characteristics. The numerically obtained flow fields will be used to (*i*) predict transport of passive chemo-attractants/repellants, (*ii*) compute the individual trajectories in the Langevin model, and (*iii*) determine the transition probabilities of the PRW model to obtain analytical predictions for transport coefficients in dilute suspension. Steps (*ii*,*iii*) directly extend the models in Aim 1.3. To realize (*i*), we will implement a multi-component reaction-diffusion-advection (RDA) model, accounting for advective and diffusive transport of chemical substances through the porous medium as well as for their potential depletion by the microorganism. Pre-computed flow fields, as shown in Fig. 6, will enter as background flows into the second-order partial differential RDA equations. The diffusion constants will be determined by the local microbial concentration [64, 40, 38] (Fig. 2H). The chemical concentration profiles obtained from these simulations will be directly tested against the microfluidic experiments of the Guasto group. Informed by the above simulations, we will fabricate additional oxygen gradient microfluidic channels (see methods section below) with specifically designed obstacle shape and spacing to maximize or minimize chemotactic motility of *B. subtilis*. Local oxygen concentrations in the cell suspensions will be measured using oxygen sensitive dye

	Tasks	Year 1				Year 2				Year 3			
		1	2	3	4	1	2	3	4	1	2	3	4
Aim 1	1.1 Design & fabricate porous microfluidic device												
	1.1 Measure cell scattering law & transport coefficients												
	1.2 High-speed flagellar & flow field measurement												
	1.3 Individual-based modeling of cell transport												
Aim 2	2.1 Determine collective motion onset in porous media												
	2.2 Extend dense suspension modeling to porous media												
	2.3 Predict & measure transport in dense suspensions												
Aim 3	3.1 Predict & measure flow effects												
	3.2 Design, fabricate & test chemotaxis microfluidic device												
	3.2 Meas. & model chemotactic transport in porous media												
	3.3 Predict & meas. effects struct. & flow on chemotaxis												

Table 1: Timeline Collaborative research activities between the Dunkel group (MIT, red) and Guasto group (Tufts, blue) over the three year project span, culminating in several highly coordinated aims (green), which will provide productive and diagnostic tools for cell motility in porous media flows.

(RTDP), and statistical metrics of cell motion will confirm simulations of the combined effects of flow and chemotaxis on cell transport.

Experimental and theoretical methods

Microfluidics PI Guasto has extensive experience designing and fabricating microfluidic devices through well-established 'soft lithography' techniques [65], performed at the Tufts Micro and Nanofabrication Facility. Molds are fabricated by patterning photoresist (SU-8-2050, MicroChem Corp.) on a silicon wafer via photolithography, where computer-generated photomasks enable precise control over microstructure and one-to-one comparison with models (Fig. 6). Nominally, the microchannels will be 4 mm $\times$ 3 cm $\times$ 10-100 μm with cylindrical obstacles (10-100 μm width), including a variety of cross-sectional shapes (e.g. circular, polygon, concave) arranged in ordered and disordered patterns (Fig. 8). Microfluidic devices are cast from silicone rubber, polydimethylsiloxane (PDMS; Sylgard 184, Dow Corning), and bonded to glass slides by exposure to oxygen plasma [24]. Microchannel surfaces are passivated with bovine serum albumen (BSA) to reduce cell sticking. Flow in the devices is controlled by a precision syringe pump (PHD Ultra 4400, Harvard Apparatus) or gravity-driven pressure difference. For chemotaxis studies (*B. subtilis*), an oxygen gradient is generated within the porous microfluidic device (Fig. 7) by adding two 300 μm-wide channels adjacent to the porous test channel, which carry nitrogen and oxygen gas, respectively. Fast oxygen diffusion from the source channel to the nitrogen channel establishes a steady, linear oxygen concentration profile, verified using oxygen-sensitive dye (RTDP) [52].

Imaging, flow measurement, and cell tracking Digital video microscopy enables direct observation and quantification of fluid flows, cell motility patterns, and flagellar mechanics. Swimming cells and passive tracer particles (0.2-1 μm), used for the flow field measurements, are observed using phase contrast microscopy (10-40$\times$, 0.3-0.65 NA) on an inverted microscope (Nikon Ti-E). A digital camera (Andor Zyla; 6.5 μm/pixel, 2560$\times$2160 pixels) captures videos (1,000-10,000 frames) of the cell and tracer motion at 30-1000 fps. Individual tracer and cell motions are extracted from video data using a predictive tracking algorithm, developed by the Guasto group (sites.tufts.edu/guastolab/movies) and implemented in parallel with Matlab on multicore workstations. Up to 10,000 cell/tracer trajectories are followed simultaneously with high accuracy through centroid or Gaussian fitting approaches ($\approx$0.1 pixel or $\leq$65 nm). Detailed measurement of the cell swimming trajectories will be characterized statistically (e.g. mean-square displacement) and

parameterized by traditional transport coefficients (e.g. diffusion coefficient), for comparison with simulations and with scalar transport theory. For individual cell flow fields, low tracer seeding is required to avoid flagellar inhibition, which necessitates particle tracking velocimetry (PTV) [21]. Flow field characterization in porous microfluidic devices is carried out similarly, where 3D flow field measurements are captured by acquiring a series of videos throughout the depth of the channel with 5 μm resolution. Collective bacterial motions are quantified using an image-based correlation method, micro-particle image velocimetry (micro-PIV) [50]. To quantify flagellar interactions with microstructured obstacles, flagella are tracked using a Gaussian fitting algorithm [Guasto *et al.*, *in prep.* (2014)]. A high-speed camera ($\geq$1000 fps) is requested to enable: (*i*) tracking of fast beating (50 Hz) eukaryotic flagella, (*ii*) unsteady flow field measurements around individual cells, and (*iii*) measurement of fast flows through porous media microfluidics.

Cell culturing and handling We will use three diverse model cells (bacterium, *Bacillus subtilis*; microalga, *Chlamydomonas reinhardtii*; human sperm), spanning key swimming styles (pusher and puller) and flagellar types (prokaryotic and eukaryotic). PI Guasto has extensive experience and his lab is fully equipped to handle all three cell types, plus a host of additional species (*Escherichia coli*, *Pseudomonas aeruginosa*) and genetic mutants, giving further control and specificity to cell morphology and swimming characteristics. Wild-type *B. subtilis* bacterial cells (OI1085) are prepared from frozen stocks by incubating in Cap Assay Minimal (CAM) motility medium at 37°C with shaking, to an optical density $\mathrm{OD}_{600} = 0.2$ (4 hr). Wild-type *C. reinhardtii* cells (cc1690) are grown in minimal medium (M1) [21, 38] at 22°C with gentle bubbling, and synchronized on a 16/8 hr bright/dark light cycle to optimize motility and size uniformity. Human sperm samples collected from healthy donors (25-45 years) are handled according to WHO guidelines [8], and prepared by the 'swim-up' method in Earle's medium [8]. Briefly, 1 mL of semen is layer on the bottom of a centrifuge tube followed by 1 mL of Earle's medium on top and incubated at 37°C. After 1 hr the top 1 mL of solution containing highly motile sperm is reserved for experiments. All experiments with bacteria, microalgae, and sperm are performed at 22°C with 0.2-0.5% BSA to further reduce sticking, and higher cell concentrations are achieved through centrifugation.

Theory and simulations To obtain quantitative predictions for the microfluidics experiments in the Guasto lab, we will simulate Stokes flow and transport equations on scales of several hundred micrometers with $>$ 100 PDMS obstacles mimicking the porous media structure (Fig. 6). Direct numerical simulation of the Stokes equation as a boundary value problem *via* Finite Element (FE) or the Finite Volume (FV) methods is numerically inefficient due to the complex boundary geometry and the large size of the microfluidic chips relative to the obstacle diameter. To overcome these limitations, the Dunkel group has implemented a penalty method that solves the modified Stokes problem (S) $0 = \nabla \cdot \boldsymbol{u}$, $0 = \mu\nabla^2\boldsymbol{u} - \nabla p - \xi\rho\boldsymbol{u}$, where $\boldsymbol{u}(\boldsymbol{x})$ is the flow velocity at position $\boldsymbol{x}$, $p(\boldsymbol{x})$ pressure and μ the dynamic viscosity. The dimensionless differentiable function $\rho(\boldsymbol{x}) \in [0, 1]$ reflects the local volume fraction of the skeletal material, with $\rho = 0$ representing voids and $\rho = 1$ obstacles, and ξ is an effective slip coefficient. Due to the absence of explicit boundaries, we can solve (S) numerically using 3D FE methods with adaptive mesh-refinement. Since (S) is linear, FE discretization leads to large but linear matrix inversion problem that is solved using Schur-type preconditioning. Adaptive error-based mesh-refinement is based on local approximation errors, whereby elements with large estimated errors are refined and elements with errors smaller than an acceptable tolerance become coarsened. The algorithm was implemented using a parallel distributed numerical solvers (P4EST and deal.ii), yielding solutions that agree very well with the corresponding experimentally measured flow fields (Fig. 6). Passive scalar and microbial transport equations will

be implemented in an analogous manner using established RDA algorithms [25].

5 Broader Impacts

Advances in our scientific understanding of swimming cell dynamics in porous media could lead to technological advances in medicine and energy with important societal implications. Such future applications could include production of clean drinking water, stifling of bacterial disease transmission, and improved efficiency of renewable biofuel production and bioremediation technologies. This award will promote an existing collaboration as well as the early career development of two productive young investigators having highly complementary expertise: PI Guasto (Tufts) is an expert in experimental biofluid dynamics, transport, and microfluidics, and PI Dunkel (MIT) is an expert in theoretical biophysics and fluid dynamics. The close proximity of MIT and Tufts will provide two Ph.D. students with a unique graduate training experience at the intersection of physics, engineering, biology, and applied math. Through monthly combined group meetings and frequent informal interactions, the student theorist and experimentalist will gain the communication skills and collaborative experience necessary for interdisciplinary careers in science and engineering. Dunkel will reserve USD4k/yr to finance one MIT PRIMES graduate mentor (USD3k/yr) and travel for one high school student (USD1k/yr). The student and graduate mentor will participate in a grant-related research project through this free, year-long after-school program for talented US high school students, offering top-level projects in mathematics, computer science, and physical and computational biology. Mentoring in PRIMES is done by MIT graduate students, who benefit from this experience by gaining advising and additional research experience, and co-authorship on resulting papers. From 2010-2014, 110 PRIMES students completed 94 research projects, resulting in presentations at the annual PRIMES conference in May and several journal publications. Leveraging numerous existing programs and the highly visual nature of their results, the PIs will broadly disseminate their work through multimedia outlets to promote STEAM, including the Cambridge Science Festival, Tufts Research Visualization Awards, and APS-DFD Gallery of Fluid Motion. The PIs consistently publish in leading scientific journals including *PNAS*, *Nature Physics*, and *Physical Review Letters*, and their work has been highlighted in popular press outlets such as *BBC News*, *Nature News and Views*, and *Physics Today*, thereby reaching a large public audience.

6 Results From Prior NSF Support

The PIs are both new faculty, and *neither PI Dunkel nor PI Guasto have received NSF funding previously.* However, PI Guasto has been supported by and has contributed to writing two successfully funded NSF grants related to multiphase flow during postdoctoral appointments. Under J.P. Gollub (Haverford Coll., DMR-0803153), PI Guasto made the first measurements of unsteady flow fields and biomixing around single cells, and investigated irreversibility in dense suspensions and the transport of elongated particles in 2D turbulence. Under R. Stocker (MIT, IOS-1120200), Guasto elucidated the trapping of swimming cells in shear, discovered a flagellar buckling mechanism in bacterial locomotion, and measured the enhanced oxygen transport in corals due to ciliary surface flows. Collectively, this work led to 9 publications (plus 2 pending) including 2 in *Nat. Phys.* [56, 52], 2 in *PNAS* [54, 38], 2 in *Phys. Rev. Lett.* [40, 21], 1 in *Phys. Rev. E* [22], 1 in *Phys. Fluids* [46], and 1 in *Ann. Rev. Fluid Mech.* [23] .

References Cited

[1] F. Azam, T. Fenchel, J. Field, J. Gray, L. Meyer-Reil, and F. Thingstad. The Ecological Role of Water-Column Microbes in the Sea. *Mar. Ecol. Prog. Ser.*, 10:257–263, 1983.

[2] M. A. Bees and O. A. Croze. Mathematics for streamlined biofuel production from unicellular algae. *Biofuels*, 5(1):53–65, 2013.

[3] H. C. Berg. *Random Walks in Biology.* Princeton University Press, Princeton, NJ, 2 edition, 1993.

[4] H. C. Berg and D. A. Brown. Chemotaxis in Ecoli. *Nature*, 239:500–504, 1972.

[5] A. P. Berke, L. Turner, H. C. Berg, and E. Lauga. Hydrodynamic Attraction of Swimming Microorganisms by Surfaces. *Phys. Rev. Lett.*, 101(3):038102, July 2008.

[6] C. Brennen and H. Winet. Fluid Mechanics of Propulsion by Cilia and Flagella. *Annu. Rev. Fluid Mech.*, 9(1):339–398, Jan. 1977.

[7] M. E. Cates. Diffusive transport without detailed balance in motile bacteria : does microbiology need statistical physics ? *Reports Prog. Phys.*, 75:042601, 2012.

[8] T. G. Cooper, editor. *WHO laboratory manual for the Examination and processing of human semen.* WHO Press, Geneva, Switzerland, 5 edition, 2010.

[9] J. P. Cowen and C. F. Holloway. Structural and chemical analysis of marine aggregates : in situ macrophotography and laser confocal and electron microscopy. *Mar. Biol.*, 126:163–174, 1996.

[10] K. Das and A. K. Mukherjee. Crude petroleum-oil biodegradation efficiency of Bacillus subtilis and Pseudomonas aeruginosa strains isolated from a petroleum-oil contaminated soil from North-East India. *Bioresour. Technol.*, 98(7):1339–45, May 2007.

[11] K. Dohnt, M. Sauer, M. Müller, K. Atallah, M. Weidemann, P. Gronemeyer, D. Rasch, P. Tielen, and R. Krull. An in vitro urinary tract catheter system to investigate biofilm development in catheter-associated urinary tract infections. *J. Microbiol. Meth.*, 87(3):302–308, Dec. 2011.

[12] C. Dombrowski, L. Cisneros, S. Chatkaew, R. E. Goldstein, and J. O. Kessler. Self-Concentration and Large-Scale Coherence in Bacterial Dynamics. *Phys. Rev. Lett.*, 93(9):098103, Aug. 2004.

[13] K. Drescher, J. Dunkel, L. H. Cisneros, S. Ganguly, and R. E. Goldstein. Fluid dynamics and noise in bacterial cell-cell and cell-surface scattering. *Proc. Natl. Acad. Sci.*, 108(27):10940–10945, 2011.

[14] K. Drescher, R. E. Goldstein, and I. Tuval. Fidelity of adaptive phototaxis. *Proc. Natl. Acad. Sci. U. S. A.*, 107(25):11171–11176, June 2010.

[15] J. Dunkel, S. Heidenreich, M. Bär, and R. E. Goldstein. Minimal continuum theories of structure formation in dense active fluids. *New J. Phys.*, 15:045016, 2013.

[16] J. Dunkel, S. Heidenreich, K. Drescher, H. H. Wensink, M. Bär, and R. E. Goldstein. Fluid Dynamics of Bacterial Turbulence. *Phys. Rev. Lett.*, 110(22):228102, May 2013.

[17] W. M. Durham, E. Climent, M. Barry, F. De Lillo, G. Boffetta, M. Cencini, and R. Stocker. Turbulenece drives microscale patches of motile phytoplankton. *Nat. Commun.*, 4:2148, 2013.

[18] W. M. Durham, J. O. Kessler, and S. Roman. Disruption of Vertical Motility by Phytoplankton Layers. *Science*, 323:1067–1070, 2009.

[19] L. J. Fauci and R. Dillon. Biofluidmechanics of Reproduction. *Annu. Rev. Fluid Mech.*, 38:371–394, 2006.

[20] P. Galajda, J. Keymer, P. Chaikin, and R. Austin. A wall of funnels concentrates swimming bacteria. *J. Bacteriol.*, 189(23):8704–8707, Dec. 2007.

[21] J. S. Guasto, K. A. Johnson, and J. P. Gollub. Oscillatory Flows Induced by Microorganisms Swimming in Two Dimensions. *Phys. Rev. Lett.*, 105:168102, Oct. 2010.

[22] J. S. Guasto, A. S. Ross, and J. P. Gollub. Hydrodynamic irreversibility in particle suspensions with nonuniform strain. *Phys. Rev. E*, 81(6):061401, June 2010.

[23] J. S. Guasto, R. Rusconi, and R. Stocker. Fluid Mechanics of Planktonic Microorganisms. *Annu. Rev. Fluid Mech.*, 44(1):373–400, Jan. 2012.

[24] K. Haubert, T. Drier, and D. Beebe. PDMS bonding by means of a portable, low-cost corona system. *Lab Chip*, 6(12):1548–1459, Dec. 2006.

[25] W. Hundsdorfer and J. G. Verwer. *Numerical Solution of Time-Dependent Advection-Diffusion-Reaction Equations*. Springer Science & Business Media, 2003.

[26] A. Jacob, E. C. Bucharsky, and K. GuenterSchell. The Application of Transparent Glass Sponge for Improvement of Light Distribution in Photobioreactors. *J. Bioprocess. Biotech.*, 02(01):1–8, 2012.

[27] G. B. Jeffery. The Motion of Ellipsoidal Particles Immersed in a Viscous Fluid. *Proc. R. Soc. London. Ser. A*, 102(715):161–179, 1922.

[28] V. Kantsler, J. Dunkel, M. Blayney, and R. E. Goldstein. Rheotaxis facilitates upstream navigation of mammalian sperm cells. *Elife*, 3:e02403–e02403, May 2014.

[29] V. Kantsler, J. Dunkel, M. Polin, and R. E. Goldstein. Ciliary contact interactions dominate surface scattering of swimming eukaryotes. *Proc. Natl. Acad. Sci. U. S. A.*, 110(4):1187–92, Jan. 2013.

[30] U. B. Kaupp and N. D. Kashikar. Mechanisms of Sperm Chemotaxis. *Annu. Rev. Physiol.*, 70:93–117, 2008.

[31] E. F. Keller and L. A. Segel. Model for chemotaxis. *J. Theor. Biol.*, 30(2):225–234, Feb. 1971.

[32] J. O. Kessler. Hydrodynamic focusing of motile algal cells. *Nature*, 313(5999):218–220, Jan. 1985.

[33] J. O. Kessler and M. Wojciechowski. *Collective Behavior and Dynamics of Swimming Bacteria*, pages 417–450. Oxford University Press, Oxford, England, 1997.

[34] F. I. Khan, T. Husain, and R. Hejazi. An overview and analysis of site remediation technologies. *J. Environ. Manage.*, 71(2):95–122, June 2004.

[35] N. Khurana and N. T. Ouellette. Interactions between active particles and dynamical structures in chaotic flow. *Phys. Fluids*, 24(9):091902, 2012.

[36] D. L. Kirchman. New light on an important microbe in the ocean. *Proc. Natl. Acad. Sci. U. S. A.*, 105(25):8487–8, June 2008.

[37] D. L. Koch and G. Subramanian. Collective Hydrodynamics of Swimming Microorganisms : Living Fluids. *Annu. Rev. Fluid Mech.*, 43:637–659, 2011.

[38] H. Kurtuldu, J. S. Guasto, K. A. Johnson, and J. P. Gollub. Enhancement of biomixing by swimming algal cells in two-dimensional films. *Proc. Natl. Acad. Sci. U. S. A.*, 108(26):10391–10395, June 2011.

[39] E. Lauga and T. R. Powers. The hydrodynamics of swimming microorganisms. *Report*, 72:096601, 2009.

[40] K. C. Leptos, J. S. Guasto, J. P. Gollub, A. I. Pesci, and R. E. Goldstein. Dynamics of Enhanced Tracer Diffusion in Suspensions of Swimming Eukaryotic Microorganisms. *Phys. Rev. Lett.*, 103:198103, 2009.

[41] G. Li and J. Tang. Accumulation of Microswimmers near a Surface Mediated by Collision and Rotational Brownian Motion. *Phys. Rev. Lett.*, 103(7):1–4, Aug. 2009.

[42] J. T. Locsei and T. J. Pedley. Run and Tumble Chemotaxis in a Shear Flow: The Effect of Temporal Comparisons, Persistence, Rotational Diffusion, and Cell Shape. *Bull. Math. Biol.*, 71:1089–1116, 2009.

[43] B. Luef, T. R. Neu, I. Zweimüller, and P. Peduzzi. Structure and composition of aggregates in two large European rivers, based on confocal laser scanning microscopy and image and statistical analyses. *Appl. Environ. Microbiol.*, 75(18):5952–62, Sept. 2009.

[44] Marcos, H. C. Fu, T. R. Powers, and R. Stocker. Bacterial rheotaxis. *Proc. Natl. Acad. Sci. U. S. A.*, 109(13):4780–4785, Mar. 2012.

[45] J. Palacci, S. Sacanna, A. P. Steinberg, D. J. Pine, and P. M. Chaikin. Living crystals of light-activated colloidal surfers. *Science*, 339(6122):936–40, Feb. 2013.

[46] S. Parsa, J. S. Guasto, M. Kishore, N. T. Ouellette, J. P. Gollub, and G. a. Voth. Rotation and alignment of rods in two-dimensional chaotic flow. *Phys. Fluids*, 23(4):043302, 2011.

[47] T. J. Pedley and J. O. Kessler. Hydrodynamic Phenomena in Suspensions of Swimming Microorganisms. *Annu. Rev. Fluid Mech.*, 24(1):313–358, Jan. 1992.

[48] M. Polin, I. Tuval, K. Drescher, J. P. Gollub, and R. E. Goldstein. Chlamydomonas Swims with Two Gears. *Science*, 325:487–490, 2009.

[49] S. Rafai, L. Jibuti, and P. Peyla. Effective viscosity of microswimmer suspensions. *Phys. Rev. Lett.*, 104:098102, 2009.

[50] M. Raffel, C. Willert, S. Wereley, and J. Kompenhans. *Particle Image Velocimetry: A practical guide*. Springer, 2 edition, 2007.

[51] J. A. Riffell and R. K. Zimmer. Sex and flow : the consequences of fluid shear for sperm – egg interactions. *J. Exp. Biol.*, 210:3644–3660, 2007.

[52] R. Rusconi, J. S. Guasto, and R. Stocker. Bacterial transport suppressed by fluid shear. *Nat. Phys.*, 10(March):212–217, 2014.

[53] J. Rutllant, M. López-Béjar, and F. López-Gatius. Ultrastructural and rheological properties of bovine vaginal fluid and its relation to sperm motility and fertilization: a review. *Reprod. Domest. Anim.*, 40(2):79–86, Apr. 2005.

[54] O. H. Shapiro, V. I. Fernandez, M. Garren, J. S. Guasto, F. P. Debaillon-Vesque, E. Karmarsky-Winter, A. Vardi, and R. Stocker. Vortical ciliary flows actively enhance mass transport in reef corals. *Proc. Natl. Acad. Sci. USA*, 111(37):13391–13396, 2014.

[55] A. Sokolov, I. S. Aranson, J. O. Kessler, and R. E. Goldstein. Concentration Dependence of the Collective Dynamics of Swimming Bacteria. *Phys. Rev. Lett.*, 158102:158102, 2007.

[56] K. Son, J. S. Guasto, and R. Stocker. Bacteria can exploit a flagellar buckling instability to change direction. *Nat. Phys.*, 9(7):1–5, July 2013.

[57] J. Taktikos, H. Stark, and V. Zaburdaev. How the Motility Pattern of Bacteria Affects Their Dispersal and Chemotaxis. *PLoS One*, 8(12):e81936, 2013.

[58] C. Torney and Z. Neufeld. Transport and Aggregation of Self-Propelled Particles in Fluid Flows. *Phys. Rev. Lett.*, 99(7):1–4, Aug. 2007.

[59] N. Tufenkji. Modeling microbial transport in porous media: Traditional approaches and recent developments. *Adv. Water Resour.*, 30(6-7):1455–1469, June 2007.

[60] I. Tuval, L. Cisneros, C. Dombrowski, C. W. Wolgemuth, J. O. Kessler, and R. E. Goldstein. Bacterial swimming and oxygen transport near contact lines. *Proc. Natl. Acad. Sci. USA*, 102(7):2277–2282, 2005.

[61] S. Uppaluri, N. Heddergott, E. Stellamanns, S. Herminghaus, A. Zöttl, H. Stark, M. Engstler, and T. Pfohl. Flow loading induces oscillatory trajectories in a bloodstream parasite. *Biophys. J.*, 103(6):1162–9, Sept. 2012.

[62] H. H. Wensink, J. Dunkel, S. Heidenreich, K. Drescher, R. E. Goldstein, H. Löwen, and J. M. Yeomans. Meso-scale turbulence in living fluids. *Proc. Natl. Acad. Sci. U. S. A.*, 109(36):14308–13, Sept. 2012.

[63] H. Wioland, F. G. Woodhouse, J. Dunkel, J. O. Kessler, and R. E. Goldstein. Confinement stabilizes a bacterial suspension into a spiral vortex. *Phys. Rev. Lett.*, 110:268102, 2013.

[64] X.-l. Wu and A. Libchaber. Particle Diffusion in a Quasi-Two-Dimensional Bacterial Bath. *Phys. Rev. Lett.*, 84:3017–3020, 2000.

[65] Y. Xia and G. M. Whitesides. Soft Lithography. *Annu. Rev. Mater. Sci.*, 28(1):153–184, Aug. 1998.

[66] A. Zöttl and H. Stark. Periodic and quasiperiodic motion of an elongated microswimmer in Poiseuille flow. *Eur. Phys. J. E*, 36(1):4, Jan. 2013.

Data Management Plan

1 Data, Software, and Other Products

The primary (raw) experimental data produced by the Tufts University team will be

1. individual cell trajectories from low concentration cell suspensions for bacteria, microalgae, and sperm
2. collective behavior of dense bacterial cell suspensions
3. tracer particle motion appropriate for image velocimetry

in the form of video and image data. Cell motility records will include bacteria, microalgae, and sperm cells swimming in an array of porous geometries fabricated in microfluidic devices and subject to a variety of hydrodynamic and chemical attractant conditions. Using quantitative image analysis techniques, the Guasto lab has generated extensive in-house cell and flagellar tracking software as well as particle tracking velocimetry (PTV) software, which is used to post-process raw video data for statistical analyses. The resulting statistical quantification will include fluid flow fields, individual cell swimming trajectories, and the flow fields characterizing the collective motion of dense bacterial suspensions.

The Dunkel group will generate source code for and data from their numerical simulations.

2 Format and Content Standards

Cell motility and flow field records are stored in the form of video (image sequence) recordings using lossless tiff images (.tif) and captured using a light microscopes equipped with digital, scientific cameras. Corresponding experimental conditions are logged in text files (.txt). Tracking and analysis codes are written in the Matlab (Mathworks, Natick, MA) scientific computing language (.m), which is a worldwide standard for image processing and analyses. The resulting statistical quantification of cell motility and fluid flow field data will be stored in Matlab data format (.mat). Simulation data will be stored in Matlab data format (.mat) or as text files (.txt).

3 Access and Sharing

The Dunkel and Guasto groups will provide access to the primary data and other supporting materials within a reasonable time. We will continue to promptly publish findings in peer-reviewed journals, in line with our strong publication record (see Biosketches), and to present at international conferences across a wide variety of disciplines (e.g., Society for Engineering Science, Society of Industrial and Applied Mathematics, American Physical Society Division of Fluid Dynamics). Select video-recorded behaviors will also be submitted to the Journal of Visualized Experiments to disseminate microfluidic channel fabrication and cell observation techniques (www.jove.com). Select videos will also be posted on YouTube, where such visual records can reach a broad audience, be freely available to the public, and be effectively used as teaching materials. Cell tracking codes will be made available through the PI website hosted at Tufts upon publication of the relevant experimental data.

4 Policies for Re-use

All unpublished materials will be freely provided upon request for reuse.

5 Archiving

Over the course of the three years of the proposed project, greater than 100 terabytes (TB) of raw video data are expected to be produced, along with the resulting statistical quantification of cell motility and flow flow field data, all of which will be archived on magnetic hard drives for at least 5 years after the completion of the project. Tracking and analysis codes are written in Matlab and are permanently archived on servers at Tufts. PI Guasto will be responsible for overseeing archiving of all raw and processed data at Tufts.